

Thermoelectric properties of electron- and hole-doped BaFe₂As₂

Y. J. Yan, X. F. Wang, R. H. Liu, H. Chen, Y. L. Xie, J. J. Ying, and X. H. Chen*

Hefei National Laboratory for Physical Science at Microscale and Department of Physics, University of Science and Technology of China, Hefei, Anhui 230026, People's Republic of China

(Received 14 January 2010; revised manuscript received 27 May 2010; published 9 June 2010)

We investigate the resistivity and thermoelectric power properties for Co- or K-doped BaFe₂As₂ systems. T_c as a function of Co- or K-doping level exhibits a domelike behavior in both of the systems. The thermoelectric power (S) at room temperature as a function of doping level (x) shows a domelike behavior in Ba_{1-x}K_xFe₂As₂ system while monotonously decreases in BaFe_{2-x}Co_xAs₂ system. It is intriguing that the superconducting samples simultaneously show large absolute values of thermoelectric power and good conductivity. The power factor shows a peak at low temperature, suggesting possible applications in thermoelectric cooling modules around the liquid-nitrogen temperature range.

DOI: 10.1103/PhysRevB.81.235107

PACS number(s): 74.25.fg, 74.25.Dw, 71.27.+a

I. INTRODUCTION

Thermoelectric properties of solids have long been a fundamental issue in condensed-matter physics and are currently attracting renewed interest because of the possibility of practical application, such as coolers (Peltier effect) and generators (Seebeck effect). The measure of their performance is the thermoelectric figure-of-merit Z which is defined as $S^2\sigma/\kappa$, where S is the thermoelectric power, σ and κ are the electronic conductivity and thermal conductivity, respectively. The power factor is defined as $P=S^2\sigma$. The most urgent need for thermoelectric applications is to find new thermoelectric materials with high ZT values around the room temperature. $ZT > 1$ is one of the criteria for practical application, although only a few semiconductors, e.g., bismuth-antimony telluride and bismuth-antimony alloys,¹ have been known to satisfy the condition. Recently, some $3d$ transition-metal oxides have drawn attention as a new category of thermoelectric materials. For example, a large Seebeck coefficient is observed at room temperature in the metallic cobalt oxide, Na_xCoO₂.² This cobalt oxide has heavy effective mass of carriers due to the strong electron-electron correlation,³ which is responsible for the large Seebeck coefficient as in some $4f$ heavy-fermion systems.⁴

Recently, large thermoelectric power has also been discovered in iron oxypnictides. Such iron oxypnictides are of ThCr₂Si₂-type structure. They adopt a layered structure with Fe layers sandwiched by two As layers with each Fe is coordinated by As tetrahedron. Similar to the cuprates, superconductivity occurs through electron or hole doping into an antiferromagnetic parent compound. Recently, the ternary iron arsenide BaFe₂As₂ shows superconductivity at 38 K by hole doping with partial substitution of K for Ba.^{5,6} In contrast to high- T_c cuprates, superconductivity can also be induced by partial substitution on Fe sites in the conducting layers by other transition-metal elements such as Co (Refs. 7–9) and Ni (Ref. 10) in the 1111 and 122 phases, and the measurements of Hall effect and thermoelectric power indicate that the electron-type charge carriers dominate in the Co-doped case.

In this paper, we report the resistivity and thermoelectric power for Co- or K-doped BaFe₂As₂ system. Thermoelectric

power measurements show large thermoelectric power in these two kinds of materials. This leads to promising thermoelectric power factors that could enable potential application of these materials in thermoelectric cooling modules around liquid-nitrogen temperatures. T_c as a function of K- or Co-doping level exhibits a domelike behavior. $S(300\text{ K})$ as a function of doping level (x) also shows a domelike behavior in Ba_{1-x}K_xFe₂As₂ system while monotonously decreases in BaFe_{2-x}Co_xAs₂ system.

II. MATERIALS AND METHODS

A series of polycrystalline Ba_{1-x}K_xFe₂As₂ samples covering from BaFe₂As₂ ($x=0$) to KFe₂As₂ ($x=1$) and a series of BaFe_{2-x}Co_xAs₂ single crystals were synthesized by solid-state-reaction method and self-flux method, respectively.^{9,11}

The samples were characterized by x-ray diffraction (XRD) using Rigaku D/max-A x-ray diffractometer with Cu $K\alpha$ radiation in the range of 10°–70° with the step of 0.02° at room temperature. The main peaks in XRD patterns of Ba_{1-x}K_xFe₂As₂ and BaFe_{2-x}Co_xAs₂ systems can be indexed using the ThCr₂Si₂-type structure with the space group I_4/mmm , indicating that the samples are almost single phase. The resistivity was measured using the standard four-probe method. The thermoelectric power was measured using a laboratory made system with a differential method.

III. RESULTS AND DISCUSSION

The resistivity for the Ba_{1-x}K_xFe₂As₂ and BaFe_{2-x}Co_xAs₂ samples is shown in Figs. 1(a) and 1(b), respectively. In these two series of samples, the anomaly associated with the structural and magnetic transition is pronounced for the low-doped samples. The anomaly is suppressed with increasing doping and in the meantime superconductivity emerges. T_c increases with further potassium or cobalt doping and reaches the maximum around $x=0.4$ and 0.2, respectively. Then, T_c begins to decrease from the maximum of about 37.5 K for the potassium doping and 25 K for the cobalt doping. At $x=1$ of potassium doping, T_c is 3.8 K for the KFe₂As₂ sample, the same as reported by Sasmal *et al.*⁶ T_c as a func-

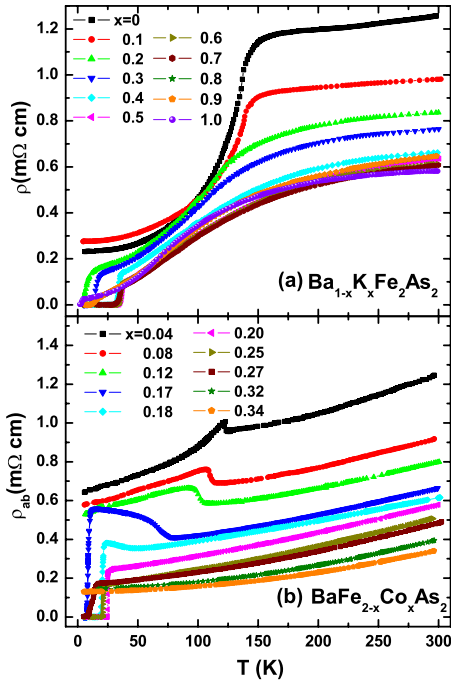


FIG. 1. (Color online) [(a) and (b)] Temperature dependence of resistivity ρ for $\text{Ba}_{1-x}\text{K}_x\text{Fe}_2\text{As}_2$ polycrystalline samples and $\text{BaFe}_{2-x}\text{Co}_x\text{As}_2$ single crystals in the temperature range from 4.2 K to 300 K, respectively (Refs. 9 and 11).

tion of Co or K doping is summarized in Figs. 2 and 3, respectively.

Temperature dependence of thermoelectric power for the $\text{Ba}_{1-x}\text{K}_x\text{Fe}_2\text{As}_2$ and $\text{BaFe}_{2-x}\text{Co}_x\text{As}_2$ samples is shown in Fig. 4. The parent compound and all the Co-doped samples show negative thermoelectric power, suggesting that electron-type carriers dominate, while all the K-doped samples show positive thermoelectric power, indicating hole-type charge carriers. When the doping level x is less than 0.1, the absolute value of thermoelectric power starts to decrease around the temperature at which the resistivity starts to decrease, as shown by the arrows in Fig. 4. Such a remarkable change in

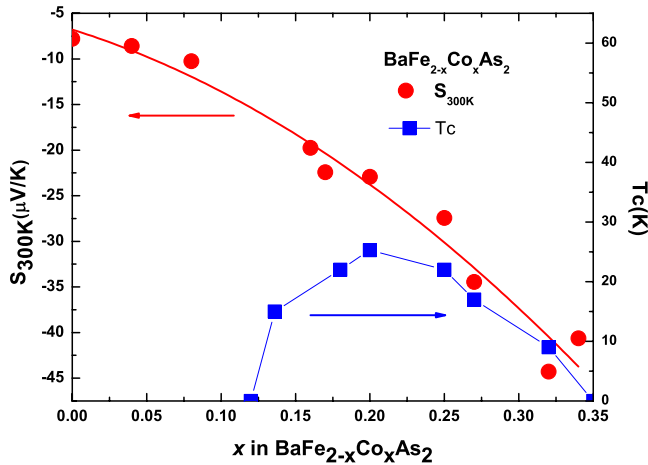


FIG. 2. (Color online) Doping dependence of room-temperature thermoelectric power, $S(300)$, for $\text{BaFe}_{2-x}\text{Co}_x\text{As}_2$. The superconducting transition temperature T_c is also shown for comparison.

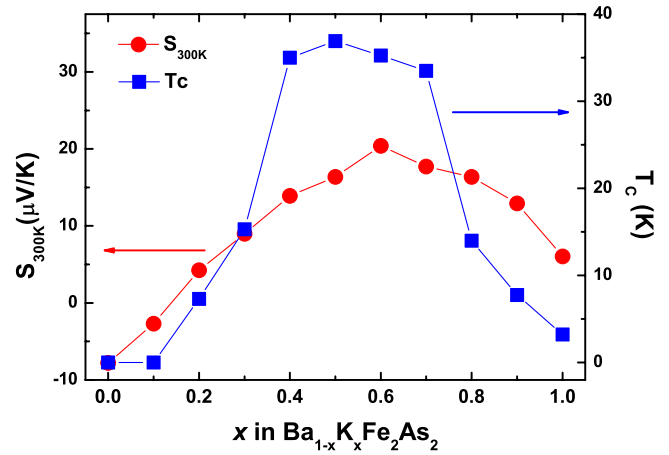


FIG. 3. (Color online) Doping dependence of room-temperature thermoelectric power, $S(300)$, for $\text{Ba}_{1-x}\text{K}_x\text{Fe}_2\text{As}_2$. The superconducting transition temperature T_c is also shown for comparison.

the thermoelectric power should be caused by the change in the electronic state when the system undergoes the structural transition and spin-density-wave (SDW) transition, and such a behavior has already been explained theoretically¹² and observed in many other compounds.^{13–15} Such behavior is gradually suppressed with increasing doping, and disappears when $x > 0.2$ in $\text{Ba}_{1-x}\text{K}_x\text{Fe}_2\text{As}_2$ system, and $x > 0.16$ in $\text{BaFe}_{2-x}\text{Co}_x\text{As}_2$ system, being consistent with the resistivity data.

For the superconducting samples, the absolute value of thermoelectric power, $|S|$, increases with decreasing tempera-

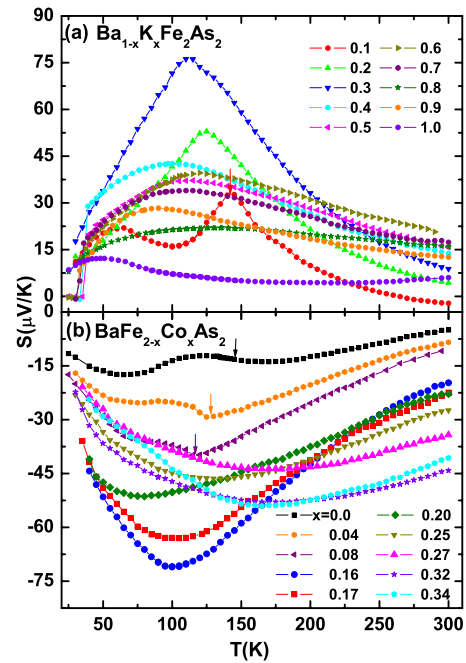


FIG. 4. (Color online) [(a) and (b)] Temperature dependence of the thermoelectric power for $\text{Ba}_{1-x}\text{K}_x\text{Fe}_2\text{As}_2$ polycrystalline samples and $\text{BaFe}_{2-x}\text{Co}_x\text{As}_2$ single crystals, respectively. The arrows in Fig. 4(b) show changes in slope arising from structural transition and SDW transition, consisting with the changes in resistivity in Fig. 1(b).

ture, while at low temperatures it develops a broad maximum which becomes broader with increasing doping. $|S|$, at around 100 K, increases quickly with K or Co doping at underdoped region, reaches a maximum of about $75 \mu\text{V}/\text{K}$, and then decreases with further doping. Such a large value of $|S|$ is very unusual in superconducting materials. However, the large $|S|$ has already been observed in F-doped $\text{LaFeAsO}_{1-x}\text{F}_x$,^{16–18} Co-doped $\text{SmFe}_{1-x}\text{Co}_x\text{AsO}$,⁸ and Ni-doped $\text{BaFe}_{2-x}\text{Ni}_x\text{As}_2$.¹⁹ It should be a universal feature for iron-based arsenide superconductors. The large thermoelectric power in superconducting region is hard to understand in conventional metal. We note that the thermoelectric power of Na_xCoO_2 is remarkably enhanced due to the electronic spin entropy.²⁰ Careful studies on the magnetic susceptibility have found that the normal-state magnetic susceptibility indeed shows a domelike doping dependence in F-doped $\text{LaFeAsO}_{1-x}\text{F}_x$ system.²¹ This susceptibility enhancement could be associated with spin fluctuations.²¹ In $\text{BaFe}_{2-x}\text{Co}_x\text{As}_2$ system, the spin fluctuations are completely suppressed when $x > 0.3$ (Ref. 22) while strong antiferromagnetic spin fluctuations are found in KFe_2As_2 .²³ Thus it suggests that the large thermoelectric power might have a magnetic origin.

It is well established that there is a universal doping (hole concentration) dependence of superconducting transition temperature, T_c , for high- T_c cuprates. Furthermore, Tallon *et al.* have found that there exists a close correlation between the room-temperature thermoelectric power, $S(290 \text{ K})$, and the hole concentration, p . A universal correlation between T_c and $S(290 \text{ K})$ is generalized in cuprate superconductors.^{24,25} In $\text{Ba}_{1-x}\text{K}_x\text{Fe}_2\text{As}_2$ and $\text{BaFe}_{2-x}\text{Co}_x\text{As}_2$ systems, we also plot the $S(300 \text{ K})$ and T_c as a function of the doping level x . In Fig. 2, $S(300 \text{ K})$ decreases monotonously with Co doping for $\text{BaFe}_{2-x}\text{Co}_x\text{As}_2$ system, while T_c as a function of Co doping shows a domelike behavior,⁹ being consistent with previous reports.²⁶ It is similar to high- T_c cuprates in which the thermoelectric power of normal state decreases monotonously with increasing doping level while T_c as a function of doping level shows a domelike behavior.^{24,25} In Fig. 3, $S(300 \text{ K})$ increases with K doping for $x > 0.1$, reaches a maximum at $x = 0.6$, and then gradually decreases with increasing x in the overdoped region in $\text{Ba}_{1-x}\text{K}_x\text{Fe}_2\text{As}_2$ system. $S(300 \text{ K})$ as a function of K doping shows a domelike behavior as T_c does.

Thermoelectric power is known to be very sensitive to the Fermi-surface (FS) topology.²⁷ Since thermoelectric power, roughly speaking, depends on the derivative of the density of states at the Fermi level, it is sensitive to subtle changes in curvature of the Fermi surface caused by the changes in carrier concentrations via K or Co doping. For a multiband system, the thermoelectric power is jointly determined by the density of states of all the bands near the Fermi level. Iron pnictides display a semimetal band structure with three hole bands and two electron bands close to the Fermi level E_F as obtained by electronic-structure calculations^{28–30} and is confirmed by angular-resolved photoemission spectroscopy.^{31,32} The change in area on holelike and electronlike Fermi surfaces goes in the opposite direction. When doping Co into electron-type BaFe_2As_2 , electron concentration monotonously increases with increasing Co content, which was con-

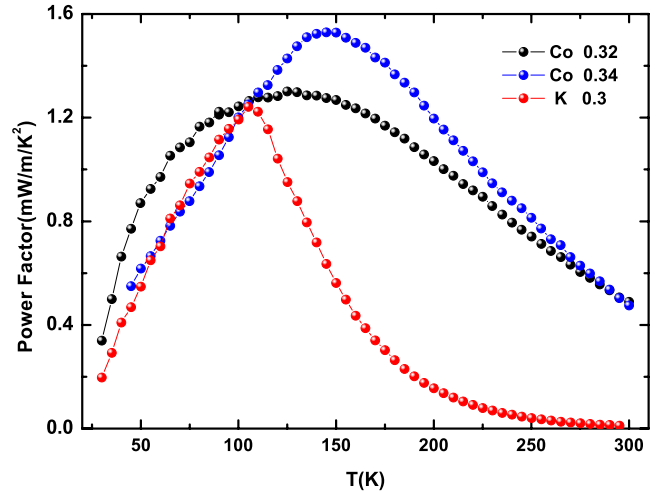


FIG. 5. (Color online) Temperature dependence of thermoelectric power factor for $\text{BaFe}_{2-x}\text{Co}_x\text{As}_2$ and $\text{Ba}_{1-x}\text{K}_x\text{Fe}_2\text{As}_2$ systems.

firmed by the Hall coefficient.^{33,34} So with Co level increasing, the area on holelike Fermi surfaces becomes smaller³⁵ and disappears at the heavy-doped region,³⁶ but the area on electronlike FSs always becomes larger, leading to a monotonic increase of $|S(300 \text{ K})|$ with Co doping. Opposite to $\text{BaFe}_{2-x}\text{Co}_x\text{As}_2$ system, when doping K into parent compound BaFe_2As_2 , the area on electronlike FSs becomes smaller³⁷ and disappears at the heavy-doped region,³⁸ but the area on holelike FSs always becomes larger. If only consider the evolution of fermi surfaces, $S(300 \text{ K})$ as a function of K doping should be a monotonic behavior. However, actually, $S(300 \text{ K})$ as a function of K-doping level exhibits more complicated behavior. One possible explanation is that there exists strong spin fluctuations in heavy-doped $\text{Ba}_{1-x}\text{K}_x\text{Fe}_2\text{As}_2$ (Ref. 23) system but not in heavy-doped $\text{BaFe}_{2-x}\text{Co}_x\text{As}_2$ (Ref. 22) system as mentioned before. To prove this, more experiments are needed.

We also report large thermoelectric power factors for the compounds studied in this family as shown in Fig. 5. The power factors reach $1.3 \text{ mW m}^{-1} \text{ K}^{-2}$ in $\text{Ba}_{0.7}\text{K}_{0.3}\text{Fe}_2\text{As}_2$ and $1.5 \text{ mW m}^{-1} \text{ K}^{-2}$ in $\text{BaFe}_{1.66}\text{Co}_{0.34}\text{As}_2$, which is the same magnitude as that in $\text{Na}_x\text{Co}_2\text{O}_4$ (Refs. 39 and 40) and Bi-Sb alloys.⁴¹ Up to now, the best thermoelectric performance in the 80–100 K temperature range is found in single-crystalline Bi-Sb alloys with a thermoelectric figure of merit ZT reaching about 0.5. The magnitude of the thermoelectric power of iron oxyphnictides is close to the best value obtained in Bi-Sb alloys.⁴¹ Meanwhile, much higher thermoelectric power values have already been reported in iron-based superconductors which have good electric conductivity. For examples, the thermoelectric power reaches $-130 \mu\text{V}/\text{K}$ in F-doped LaFeAsO , $-100 \mu\text{V}/\text{K}$ in F doped NdFeAsO ,^{16–18} and $-80 \mu\text{V}/\text{K}$ in Co-doped SmFeAsO ,⁸ leading to much higher power factors. And also, we note that the values of resistivity are obtained in $\text{Ba}_{1-x}\text{K}_x\text{Fe}_2\text{As}_2$ polycrystalline samples that are not very dense, thus an improvement in this aspect can easily be made.

On the other hand, it has been reported that hole doping on the rare-earth oxide layer or Fe-As layer can yield p -type materials. This would be of fundamental interest for applica-

tions since the thermoelectric properties of the known p -type compounds are rather poor at low temperature. Furthermore, we can simultaneously find n -type and p -type materials with large thermoelectric power in the same kind of iron oxypnictides, showing that iron oxypnictides will be good candidates for thermoelectric cooling applications in the liquid-nitrogen temperature range.

IV. CONCLUSION

In conclusion, the transport properties for Co-doped $\text{BaFe}_{2-x}\text{Co}_x\text{As}_2$ system and K-doped $\text{Ba}_{1-x}\text{K}_x\text{Fe}_2\text{As}_2$ exhibit systematic evolution with Co- and K-doping level, respectively. Combining resistivity and thermoelectric power, we can see that SDW order is quickly suppressed and superconductivity emerges by Co or K doping. Phase diagrams are derived based on the transport measurements and a domelike

behavior for T_c as a function of x (K- or Co-doping content) is established. Furthermore, $|S(300\text{ K})|$ as a function of x in $\text{Ba}_{1-x}\text{K}_x\text{Fe}_2\text{As}_2$ also shows a domelike behavior as $T_c(x)$ does while it evolves monotonously in $\text{BaFe}_{2-x}\text{Co}_x\text{As}_2$ system. The difference between the two systems may be caused due to the different evolution of the Fermi surfaces and the intensity of spin fluctuations. Besides, the large thermoelectric power factors in iron-oxypnictide materials indicate potential applications in thermoelectric cooling modules around liquid-nitrogen temperatures.

ACKNOWLEDGMENTS

This work is supported by the Nature Science Foundation of China and by the Ministry of Science and Technology of China (973 Project No. 2006CB601001) and by National Basic Research Program of China (Grant No. 2006CB922005).

*Corresponding author; chenxh@ustc.edu.cn

- ¹G. D. Mahan, B. Sales, and J. Sharp, *Phys. Today* **50**(3), 42 (1997).
- ²I. Terasaki, Y. Sasago, and K. Uchinokura, *Phys. Rev. B* **56**, R12685 (1997).
- ³Y. Ando, N. Miyamoto, K. Segawa, T. Kawata, and I. Terasaki, *Phys. Rev. B* **60**, 10580 (1999).
- ⁴G. Pálsson and G. Kotliar, *Phys. Rev. Lett.* **80**, 4775 (1998).
- ⁵G. Wu, R. H. Liu, H. Chen, Y. J. Yan, T. Wu, Y. L. Xie, J. J. Ying, X. F. Wang, D. F. Fang, and X. H. Chen, *EPL* **84**, 27010 (2008).
- ⁶K. Sasmal, B. Lv, B. Lorenz, A. M. Guloy, F. Chen, Y. Y. Xue, and C. W. Chu, *Phys. Rev. Lett.* **101**, 107007 (2008).
- ⁷A. S. Sefat, A. Huq, M. A. McGuire, R. Jin, B. C. Sales, D. Mandrus, L. M. D. Cranswick, P. W. Stephens, and K. H. Stone, *Phys. Rev. B* **78**, 104505 (2008).
- ⁸C. Wang, Y. K. Li, Z. W. Zhu, S. Jiang, X. Lin, Y. K. Luo, S. Chi, L. J. Li, Z. Ren, M. He, H. Chen, Y. T. Wang, Q. Tao, G. H. Cao, and Z. A. Xu, *Phys. Rev. B* **79**, 054521 (2009).
- ⁹X. F. Wang, T. Wu, G. Wu, R. H. Liu, H. Chen, Y. L. Xie, and X. H. Chen, *New J. Phys.* **11**, 045003 (2009).
- ¹⁰G. Cao, S. Jiang, X. Lin, C. Wang, Y. Li, Z. Ren, Q. Tao, C. Feng, J. Dai, Z. Xu, and F. C. Zhang, *Phys. Rev. B* **79**, 174505 (2009).
- ¹¹H. Chen, Y. Ren, Y. Qiu, Wei Bao, R. H. Liu, G. Wu, T. Wu, Y. L. Xie, X. F. Wang, Q. Huang, and X. H. Chen, *EPL* **85**, 17006 (2009).
- ¹²L. L. Van Zandt and A. W. Overhauser, *Phys. Rev.* **141**, 583 (1966).
- ¹³E. Fawcett, H. L. Alberts, V. Yu. Galkin, D. R. Noakes, and J. V. Yakhmi, *Rev. Mod. Phys.* **66**, 25 (1994).
- ¹⁴K. Saito, H. Yoshino, K. Kikuchi, K. Kobayashi, and I. Ikemoto, *J. Phys. Soc. Jpn.* **62**, 1001 (1993).
- ¹⁵V. A. Bondarenko, S. Kagoshima, M. Maesato, T. Hasegawab, N. Miurac, and T. Yamaguchid, *Synth. Met.* **103**, 2218 (1999).
- ¹⁶L. Pinsard-Gaudart, D. Brardan, J. Bobroff, and N. Drago, *Phys. Status Solidi (RRL)* **2**, 185 (2008).
- ¹⁷A. S. Sefat, M. A. McGuire, B. C. Sales, R. Jin, J. Y. Howe, and D. Mandrus, *Phys. Rev. B* **77**, 174503 (2008).
- ¹⁸M. A. McGuire, A. D. Christianson, A. S. Sefat, B. C. Sales, M. D. Lumsden, R. Jin, E. A. Payzant, D. Mandrus, Y. Luan, V. Keppens, V. Varadarajan, J. W. Brill, R. P. Hermann, M. T. Sougrati, F. Grandjean, and G. J. Long, *Phys. Rev. B* **78**, 094517 (2008).
- ¹⁹L. J. Li, Q. B. Wang, Y. K. Luo, H. Chen, Q. Tao, Y. K. Li, X. Lin, M. He, Z. W. Zhu, G. H. Cao, and Z. A. Xu, *New J. Phys.* **11**, 025008 (2009).
- ²⁰G. Caro, B. Bourdon, J.-L. Birck, and S. Moorbath, *Nature (London)* **423**, 428 (2003).
- ²¹T. Nomura, S. W. Kim, Y. Kamihara, M. Hirano, P. V. Sushko, K. Kato, M. Takata, A. L. Shluger, and H. Hosono, *Supercond. Sci. Technol.* **21**, 125028 (2008).
- ²²F. L. Ning, K. Ahilan, T. Imai, A. S. Sefat, M. A. McGuire, B. C. Sales, D. Mandrus, P. Cheng, B. Shen, and H. H. Wen, *Phys. Rev. Lett.* **104**, 037001 (2010).
- ²³S. W. Zhang, L. Ma, Y. D. Hou, J. Zhang, T. L. Xia, G. F. Chen, J. P. Hu, G. M. Luke, and W. Yu, *Phys. Rev. B* **81**, 012503 (2010).
- ²⁴S. D. Obertelli, J. R. Cooper, and J. L. Tallon, *Phys. Rev. B* **46**, 14928 (1992).
- ²⁵J. L. Tallon, C. Bernhard, H. Shaked, R. L. Hitterman, and J. D. Jorgensen, *Phys. Rev. B* **51**, 12911 (1995).
- ²⁶E. Mun, S. Bud'ko, N. Ni, and P. Canfield, [arXiv:0906.1548](https://arxiv.org/abs/0906.1548) (unpublished).
- ²⁷P. Li, K. Behnia, and R. L. Greene, *Phys. Rev. B* **75**, 020506(R) (2007).
- ²⁸D. J. Singh, *Phys. Rev. B* **78**, 094511 (2008).
- ²⁹I. I. Mazin and J. Schmalian, *Physica C* **469**, 614 (2009).
- ³⁰F. Ma, Z. Lu, and T. Xiang, *Fron. Phys. China* **5**, 150 (2010).
- ³¹D. Hsieh, Y. Xia, L. Wray, D. Qian, K. Gomes, A. Yazdani, G. Chen, J. Luo, N. Wang, and M. Hasan, [arXiv:0812.2289](https://arxiv.org/abs/0812.2289) (unpublished).
- ³²M. Yi, D. H. Lu, J. G. Analytis, J. H. Chu, S. K. Mo, R. H. He, R. G. Moore, X. J. Zhou, G. F. Chen, J. L. Luo, N. L. Wang, Z. Hussain, D. J. Singh, I. R. Fisher, and Z. X. Shen, *Phys. Rev. B* **80**, 024515 (2009).

- ³³F. Rullier-Albenque, D. Colson, A. Forget, and H. Alloul, *Phys. Rev. Lett.* **103**, 057001 (2009).
- ³⁴Lei Fang, Huiqian Luo, Peng Cheng, Zhaosheng Wang, Ying Jia, Gang Mu, Bing Shen, I. I. Mazin, Lei Shan, Cong Ren, and Hai Hu Wen, *Phys. Rev. B* **80**, 140508(R) (2009).
- ³⁵K. Terashima, Y. Sekiba, J. H. Bowen, K. Nakayama, T. Kawahara, T. Sato, P. Richard, Y.-M. Xu, L. J. Li, G. H. Cao, Z.-A. Xu, H. Ding, and T. Takahashi, *Proc. Natl. Acad. Sci. U.S.A.* **106**, 7330 (2009).
- ³⁶Y. Sekiba, T. Sato, K. Nakayama, K. Terashima, P. Richard, J. H. Bowen, H. Ding, Y.-M. Xu, L. J. Li, G. H. Cao, Z.-A. Xu, and T. Takahashi, *New J. Phys.* **11**, 025020 (2009).
- ³⁷H. Ding, P. Richard, K. Nakayama, K. Sugawara, T. Arakane, Y. Sekiba, A. Takayama, S. Souma, T. Sato, T. Takahashi, Z. Wang, X. Dai, Z. Fang, G. F. Chen, J. L. Luo, and N. L. Wang, *EPL* **83**, 47001 (2008).
- ³⁸T. Sato, K. Nakayama, Y. Sekiba, P. Richard, Y.-M. Xu, S. Souma, T. Takahashi, G. F. Chen, J. L. Luo, N. L. Wang, and H. Ding, *Phys. Rev. Lett.* **103**, 047002 (2009).
- ³⁹M. Ito, T. Nagira, and S. Hara, *J. Alloys Compd.* **408-412**, 1217 (2006).
- ⁴⁰T. Seetawan, V. Amornkitbamrung, T. Burinprakhon, S. Maensiri, K. Kurosaki, H. Muta, M. Uno, and S. Yamanaka, *J. Alloys Compd.* **407**, 314 (2006).
- ⁴¹H. Kitagawa, Hiroyuki Noguchi, Toshiyasu Kiyabu, Masaki Itoh, and Yasutoshi Noda, *J. Phys. Chem. Solids* **65**, 1223 (2004).